Deep-Sea Research, Vol. 37, No. 3, pp. 431–446, 1990.
Printed in Great Britain.

0198–0149/90 $3.00 + 0.00

Convection from a source in an ocean basin

KEVIN SPEER*† and ELI TZIPERMAN‡

(*Received* 13 *January* 1989; *in revised form* 30 *July* 1989; *accepted* 23 *October* 1989)

Abstract—A model is presented for the deep interior stratification and upwelling in an ocean basin connected to a marginal sea. Three elements make up the model: a marginal sea, a turbulent boundary current and an interior region. The system is subject to rotation. Once the forcing by an air–sea heat flux at the surface of the marginal sea is specified, the amount of dense water formed, the structure and trajectory of the boundary current carrying this water along a sloping bottom to the deep ocean, and the interior stratification can be calculated. As the boundary current flows along the bottom, it first entrains the surrounding water and its density decreases. When the density of the boundary current approaches that of the interior, near the bottom of the ocean, the current detrains and looses its water to the interior. Mass continuity for the interior requires the interior upwelling velocity to increase away from the bottom and then decrease at the levels where the boundary current entrains interior water. The interior density profile looks exponential although the interior upwelling varies with depth. The horizontal circulation implied by this vertical velocity profile and the large-scale linear vorticity equation is like that of STOMMEL and ARONS (1960, *Deep-Sea Research*, **6**, 140–154) near the bottom, while at mid-depth the flow has the same pattern but moves in the opposite direction. An example with sloping interior walls is given, and the effect of rotation on the stratification is discussed.

1. INTRODUCTION

THE circulation in the ocean is driven by air–sea fluxes of momentum, heat and salt at the surface of the ocean. The response to these fluxes is not limited to the surface because the dense water formed by these fluxes moves toward the ocean's interior. It is our purpose to show how air–sea interaction in limited regions of dense water formation affects the deep interior of the ocean. The role of bottom boundary currents carrying water masses from their formation sites to the deep interior, and the connection between these currents and the ocean's interior are also addressed.

The difficulties in relating air–sea fluxes to the deep interior, through bottom boundary currents have led previous efforts to concentrate on only one or two of the three, and to ignore the rest. SMITH (1975) described a model of bottom boundary currents representing the outflow of heavy water at shallow sills separating the ocean interior from the marginal basins. He was able to reproduce the downstream evolution of average cross-sectional

* Woods Hole Oceanographic Institution, Woods Hole, MA 02543, U.S.A.
† Present address: Meeresphysik, Institut für Meereskunde, Dürstenbrooker Weg 20, D2300 Kiel, Germany.
‡ Isotopes Department, The Weizmann Institute of Science, Rehovot, 76100, Israel.

properties in the boundary currents resulting from the flow through the Denmark Strait and the Mediterranean outflow. KILLWORTH (1977) extended Smith's work to include the effects of pressure on the thermal expansion coefficient, in order to model the water mass formation at the Weddell Sea continental slope. In both works, the heavy water sinks because of the difference between its density and that of the surrounding water, but the density of the surrounding water had to be specified and was not found as part of the solution.

GARGETT (1984) presented a simple model for the deep circulation, in which the interior velocity is calculated from the density profile, using the vertical density equation with vertical mixing coefficient that depends on the vertical stratification. Again, the density profile is specified rather than calculated by the model. TZIPERMAN (1986) related the deep interior stratification and circulation to air–sea fluxes through the formation of deep water masses, but ignored the mixing affecting these water masses on their way from formation regions to the deep interior.

MANINS (1979) has extended the work of BAINES and TURNER (1969), who presented the fundamental idea of the coupling between the boundary current structure and the interior structure in a confined non-rotating system, by presuming the existence of a steady state in which the fluxes of buoyancy and mass carried downward by the boundary current are balanced by interior diffusion and upwelling.

Here all three components are included: a simple heat balance equation for a marginal sea where dense water is formed, a turbulent boundary current carrying this water to the bottom, and diffusion in the interior to balance uniform upwelling. The present model can be seen as an extension of the convection problem with a point source of buoyancy discussed by MANINS (1979). The major differences here are the addition of rotation, which is crucial for the large-scale oceanic problem, and also the treatment of detrainment of the boundary current into the interior. This latter aspect is discussed further in Section 3.

In the following sections first the model is described (2), then the results of an example run motivated by the Denmark Strait outflow and the North Atlantic Ocean are presented (3). This is compared to simpler cases without rotation, and then an example is shown with topography, followed by some discussion (4).

2. THE MODEL

The model (Fig. 1) has three main components: a marginal sea, where deep water is formed by intense surface cooling; a bottom boundary current, carrying the dense water from the marginal sea outflow to the bottom of the ocean while entraining interior water on the way to the bottom; and the deep (below thermocline) interior of the ocean, where a uniform upwelling returns the deep water back to the upper ocean. It is assumed that in the upper part of the interior (not modeled), water flows back to the marginal sea, thus closing the circulation. The depth of the marginal sea's sill is, by assumption, equal to the depth of the top of the interior that is explicitly included in the model. With the North Atlantic Ocean as an example, the above three components are meant to schematically represent the Norwegian Sea, the Denmark Strait outflow and the interior of the North Atlantic Ocean.

The outflow is driven down the sloping bottom by the density difference between it and the surrounding interior water. Its evolution and final depth of penetration are, therefore,

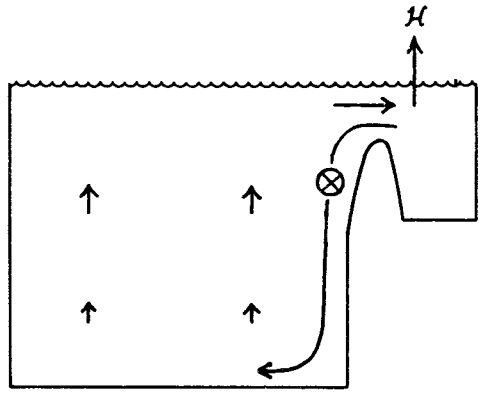

Fig. 1. A schematic view of the model, showing the marginal sea connected to the interior through a sill, and the boundary current carrying water from the marginal sea to the bottom of the interior.

affected by the interior density profile. On the other hand, the current entrains interior water while flowing down the slope, and later, near the bottom, loses its water to the interior; through these exchanges the current affects the interior stratification and circulation.

Details of the three model components

The bottom boundary current is modeled by a "streamtube" model as by SMITH (1975) and KILWORTH (1977), with some extensions necessary for our purposes. The density and velocity of the boundary current, assumed uniform in cross-section, are denoted by ρ and V. The cross-section area of the current is A, the distance along the axis of the tube is ξ, and ρ_e is the density of the interior water. The equations for mass (volume) and internal energy (buoyancy) conservation for the tube, written in flux form are (SMITH, 1975)

$$\frac{\mathrm{d}(AV)}{\mathrm{d}\xi} = E_0 A^{1/2} V - P_M, \tag{1}$$

$$\frac{\mathrm{d}(\rho AV)}{\mathrm{d}\xi} = \rho_e E_0 A^{1/2} V - \rho_e P_M - \kappa(\rho - \rho_e), \tag{2}$$

where

$$P_M = \frac{A\rho_0}{2\tau\,\delta\rho} \exp\left(-\frac{|\rho - \rho_e|}{\delta\rho}\right). \tag{3}$$

The term $E_0 A^{1/2} V$ represents the entrainment of interior water by the boundary current, assumed proportional to the velocity times width, with proportionality constant E_0 (KILLWORTH, 1977). The term P_M is added in the present model to represent the detrainment of tube water into the interior, and its form (3), is derived in the Appendix. When the boundary current density is significantly larger than the interior density, the detrainment is negligible, while when the two get closer, P_M becomes larger and the

boundary current loses its water to the interior. The last term in (2) represents horizontal mixing without any net mass exchange. From (1) and (2),

$$\rho_\xi = -\frac{\Delta\rho M}{AV} - \frac{\kappa}{AV},$$

where $M = E_0 A^{1/2} V - P_M$ is the total mass gained by the current from the interior, and $\Delta\rho = \rho - \rho_e$. The κ term prevents the plume's density from increasing when it loses water ($M < 0$).

As it flows down the slope, the current is deflected to the right in the northern hemisphere by the Coriolis force. Following Smith's notation (Fig. 2), the angle between a level surface and the slope is α, the distance down the slope is y, and the perpendicular axis marking distance along the isobaths is x. The angle between the axis of the current and the x-axis is β, so that

$$\frac{dx}{d\xi} = \cos(\beta), \qquad \frac{dy}{d\xi} = \sin(\beta).$$

The equations for the momentum components perpendicular and parallel to the tube axis are

$$\rho V\left(f + V\frac{\partial\beta}{\partial\xi}\right) = sg\,\Delta\rho\cos(\beta), \tag{4}$$

$$\frac{d}{d\xi}(\rho A V^2) = sg\,\Delta\rho A\sin(\beta) - \rho K_0 A^{1/2} V^2, \tag{5}$$

where K_0 is a bottom friction coefficient and $s = \tan(\alpha)$.

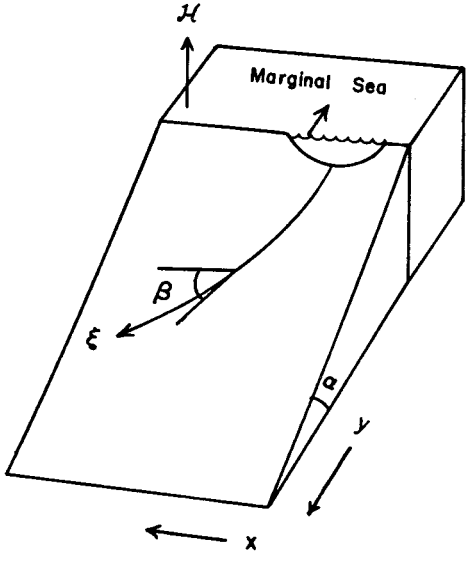

Fig. 2. The geometry of the streamtube model for the boundary current carrying the water from the marginal sea to the ocean interior.

The interior upwelling arises because of the downward boundary current transport. Conservation of mass requires that the vertical transport of the boundary current at each level is equal to the total upwelling at that level

$$A(z)V(z) = \iint_{\text{interior}} w \, dx \, dy = A_I(z)w(z),$$

or

$$w(z) = A(z)V(z)/A_I(z), \tag{6}$$

where A_I is the interior area of the ocean (and A_I is much greater than A). In most examples to follow, A_I is constant.

It is assumed here that the isopycnal surfaces in the ocean interior are flat, and so the interior density is a function of the vertical coordinate z only,

$$\rho_e = \rho_e(z).$$

A horizontal integration of the full density advection–diffusion equation over the interior up to the edge of the boundary current together with (2) gives

$$w\rho_{ez} = \kappa_v \rho_{ezz} - \frac{\kappa}{A_I} \Delta\rho, \tag{7}$$

where the upwelling velocity w is therefore also horizontally uniform. The assumption of horizontally uniform density field can be also supported by dynamical considerations (TZIPERMAN, 1986) and the use of the vertical density equation (7, without the κ term) can be justified by simple scaling arguments (WARREN, 1977). The form of the horizontal mixing term in (7) was chosen to cancel the same from (2) to obtain the total density flux equation

$$\kappa_v \rho_{ez} = -w \, \Delta\rho \tag{8}$$

representing the steady-state balance of density in the basin. This equation comes from combining (1), (2), (6) and (7) and integrating. The horizontal circulation of the interior will be discussed later.

The marginal sea is represented here by a simple heat balance equation. The air–sea heat flux $\mathcal{H}$ in the marginal sea is specified, and is related to the transport AV of water passing through the marginal sea and the density of the inflow and outflow water by

$$AV(\rho_{\text{in}} - \rho_{\text{out}}) = \frac{\alpha'}{C_p} \mathcal{H}, \tag{9}$$

where α' and C_p are the thermal expansion coefficient and specific heat, respectively.

Equations (1–6) can be written as an initial value problem with the distance along the current, ξ, replacing time. To do so, define $r = \rho_{ez}$, and nondimensionalize the equations using the scaling

$$x, y \sim L \qquad V \sim U = \sqrt{g'L} \qquad w \sim \frac{UL^2}{A_I} \qquad \kappa \sim UL \qquad Ro = \frac{U}{fL} \qquad P_e = \frac{L^2}{A_I} \frac{UL}{\kappa_v},$$

where $g' = 1$ cm s^{-2}, and $L = 1$ km.

The governing equations for the boundary current and the interior are then

$$\begin{aligned}
A_\xi &= -\sin(\alpha)\sin(\beta)A\,\Delta\rho/V^2 + 2(E_0\sqrt{A} - P_M/V) + K_0\sqrt{A} \\
V_\xi &= \sin(\alpha)\sin(\beta)\,\Delta\rho/V - V(E_0 + K_0)/\sqrt{A} + P_M/A \\
\rho_\xi &= -(E_0\sqrt{A} - P_M/V + \kappa/V)\,\Delta\rho/A \\
\rho_{e\xi} &= -\sin(\alpha)\sin(\beta)r \\
r_\xi &= -P_e\sin(\alpha)\sin(\beta)wr + P_e\kappa\,\Delta\rho \\
\beta_\xi &= \sin(\alpha)\cos(\beta)\,\Delta\rho/V^2 - Ro^{-1}/V \\
x_\xi &= \cos(\beta) \\
y_\xi &= \sin(\beta),
\end{aligned} \tag{10}$$

where we also used $z = y\sin(\alpha)$ and $\mathrm{d}/\mathrm{d}z = -(\sin(\alpha)\sin(\beta))^{-1}\,\mathrm{d}/\mathrm{d}\xi$ to derive (10). Where density is not differentiated it has been set to one.

Once the initial values of all variables at sill depth, $\xi = 0$ are specified, (10) can be stepped forward to solve for their values for all ξ. To finish posing the problem, we need to discuss the boundary conditions and matching conditions between the different model components. These matching conditions will be used to calculate the initial conditions for all variables in (10).

Boundary and matching conditions

To solve (10), the interior gradient of density, ρ_{ez}, needs to be specified at $\xi = 0$. Note that with the boundary current as the only source of deep water, density (internal energy) conservation requires that the density transport of the boundary current be equal to that of the interior at $\xi = 0$

$$\iint_{\text{interior}} w\rho_e - \kappa_V\rho_{ez}\,\mathrm{d}x\,\mathrm{d}y = \rho AV \qquad \text{at } \xi = 0,$$

or

$$r \equiv \rho_{ez} = \frac{w\rho_e - (\rho AV)/A_I}{\kappa_V} \qquad \text{at } \xi = 0. \tag{11}$$

Since the boundary current is, by assumption, the only source of bottom water to the interior, its density when reaching the bottom must be equal to the interior density at the bottom

$$\rho = \rho_e \qquad \text{at } z_{\text{bot}}. \tag{12}$$

This is the matching condition between the boundary current and the interior. If it is not satisfied, and the boundary current reaches the density of the interior before reaching the bottom, the current will stop sinking and spread horizontally, leaving the interior with no source of bottom water. If, on the other hand, the interior bottom water is lighter than the boundary current water (which is its source) the model is again inconsistent.

Finally, the marginal sea equation (9) is matched to the interior and to the boundary current models. The net transport into the marginal sea AV is equal to the initial transport

of the boundary current, $A(\xi = 0)\, V(\xi = 0)$, while the densities of the water entering and leaving the marginal sea are equal to the interior density and boundary current density at $\xi = 0$, respectively. Rewriting (9) we have

$$AV(\rho_e - \rho) = \frac{\alpha'}{C_p}\,\mathcal{H} \qquad \text{at } \xi = 0. \tag{13}$$

This completes the formulation of the model, and we proceed to solve for the interior and boundary current evolution. First, the values of all variables at $\xi = 0$ are calculated using the above relations and boundary conditions. The initial cross-section area of the boundary current $A(\xi = 0)$ and the initial interior density $\rho_e(\xi = 0)$ must be specified (the initial area can be regarded as the cross-section area of the sill connecting the interior and the marginal sea). Temporarily, the density of the outflow $\rho(\xi = 0)$ is specified, and it will be calculated later as part of the solution. Next, given A, ρ, ρ_e at $\xi = 0$, the density balance for the marginal sea (13) is used to find the boundary current initial velocity $V(\xi = 0)$. Then we use the mass conservation condition (6) to calculate the interior upwelling velocity w at $\xi = 0$ and interior density conservation (11) to find the initial value of $r = \rho_{ez}$. Finally, the coordinates (x, y) are chosen so that the outflow begins at (0, 0) and the current starts flowing down the slope: $\beta(\xi = 0) = \pi/2$.

Having the initial values of all variables, their values for all ξ can be calculated by stepping (10) forward in ξ. This is done using a Runge–Kutta method (Shampine *et al.*, 1975).

As the matching condition (12) between the densities of the boundary current and the interior at z_{bot} is not yet applied, it probably will not be satisfied by the solution. The initial outflow density $\rho(\xi = 0)$, arbitrarily specified before, can now be varied until the correct value is found and the above matching condition is satisfied, completing the solution for all variables of the model.

We want to emphasize that the only quantities specified, apart from the geometry of the model, are the air–sea heat flux in the marginal sea $\mathcal{H}$ and the inflow density. If in addition the heat flux is proportional to the air–sea temperature difference, then these two quantities are not independent, and we really only have one specified quantity. All other variables—in particular the interior and boundary current density profiles and velocity profiles—are determined by the model.

3. EXAMPLES

Figure 3 shows a calculation motivated by the Norwegian Sea outflow. The parameters used are as follows. For the marginal sea equation (13), the heat flux is taken from Worthington (1970), $\mathcal{H} = 2.52 \times 10^{14}$W; a near-surface value is used for the expansion coefficient $\alpha' = 6.6 \times 10^{-5}\ ^\circ\text{C}^{-1}$ and $C_p = 3.99\ \text{J g}^{-1}\ ^\circ\text{C}^{-1}$ (Gill, 1982), so that the right-hand side of (13) is 1.32 when scaled. In the interior the vertical mixing coefficient is $\kappa_v = 1.7\ \text{cm}^2\,\text{s}^{-1}$, and the interior area is $A_I = 2.5 \times 10^7\ \text{km}^2$. For the boundary current the initial cross-section $A(\xi = 0) = 8\ \text{km}^2$, the entrainment and friction coefficients (1, 2) are $E_0 = 0.0005$ and $K_0 = 0.11$, the detrainment parameters (3) are $\delta\rho = 0.01 \times 10^{-3}\text{g cm}^{-3}$, $\tau = 10^4$, and κ is set to $1.1P_M$ when the current loses water ($M < 0$). The κ term is only important in the 100–200 m above the bottom, where w becomes small. These values of E_0 and K_0 are similar to those of Smith (1975, Table 4) for which E_0 was either 6.5×10^{-4}

or 10^{-3} and K_0 was either 0.01 or 0.15, and those of KILLWORTH (1979, Fig. 8) for which $E_0 = 1.5 \times 10^{-4}$ and $K_0 = 0.15$. The Coriolis parameter $f = 1.4 \times 10^{-4}\,s^{-1}$.

The trajectory of the boundary current along the sloping bottom (Fig. 3a) shows the deflection of the current to the right by the Coriolis force. The density profiles (Fig. 3b) of the current (full line) and interior (dashed) approach each other with increasing depth, and meet at the ocean's bottom. Note that although the interior density profile looks exponential, and the interior mixing coefficient is constant, the vertical velocity is not constant but varies greatly with depth (Fig. 3c). The nondimensional depth scale for the interior density variation $d = \Delta\rho/r = \Delta\rho/P_e(\alpha'\mathcal{H})/(C_p)$ becomes $d \simeq \Delta\rho$ for the parameters chosen, which indicates a depth of about 2 km.

The vertical velocity profile when scaled is equal to that of the transport of the boundary

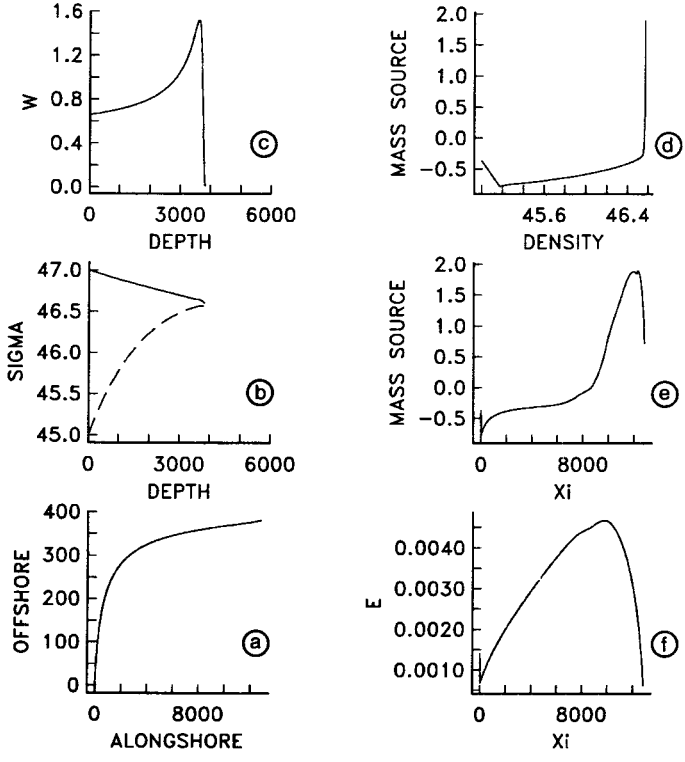

Fig. 3. Result of the example model run described in Section 3. Distance from the shore in km, depth is m. The vertical velocity W is in units of 1.3×10^{-5} cm s^{-1}, density in σ-notation kg m^{-3}. (a) The trajectory of the bottom boundary current along the bottom. (b) The density of the bottom boundary current (full line) and of the interior water (dash line), as function of depth. (c) The interior vertical velocity as function of depth, which is also the profile of the transport of the boundary current. (d) The interior mass source $-M$ (m^2 s^{-1}) vs interior density. (e) The mass source M vs ξ. (f) The entrainment term $E = E_0 A^{1/2} V$ vs ξ. The vertical velocity is zero at the bottom, it then increases as a result of the bottom water supplied by the detraining boundary current. At higher levels, the upwelling velocity decreases again owing to the entrainment of interior water by the boundary current. The interior circulation deduced from this profile is northward near the bottom, and southward in the upper levels. In practice, the plume was considered to have reached the bottom if it got to within 200 m of 4000 m depth.

current as a function of depth. As it flows out of the marginal sea, the current first entrains interior water, thereby increasing its transport, and later (below about 3500 m) loses its water to the interior. These changes correspond to an initial increase of the vertical velocity above the bottom, and then a decrease from 3500 m to the top. They occur fairly gradually along the track, but over most of its density range the interior is losing mass (Fig. 3d). The water leaving the current near the bottom is made up of roughly one-half densified Norwegian Sea water and one-half entrained water.

The interior circulation can be calculated from the vertical velocity profile using the linear vorticity equation $\hat{\beta}v = fw_z$, where f is the Coriolis parameter, $\hat{\beta}$ is its derivative with respect to latitude, and v is the interior meridional velocity (WARREN, 1981). The interior vertical velocity profile in Fig. 3c induces, therefore, a southward mid-depth interior circulation above 3500 m, where $w_z < 0$, and a northward circulation in the layer near the bottom, below 3500 m depth.

The vertically integrated circulation in the bottom layer, below about 3500 m, is identical to that of STOMMEL and ARONS' (1960) model, but note that in the present model one also obtains the vertical structure of this circulation by specifying only the surface forcing $\mathcal{H}$. The streamlines of the southward circulation above 3500 m are similar to those below, in the bottom layer, except that the direction of flow is reversed. The transport carried by the mid-depth circulation is proportional to the vertical velocity difference across this layer, and is about a third of the transport of the bottom layer (Fig. 3c). The

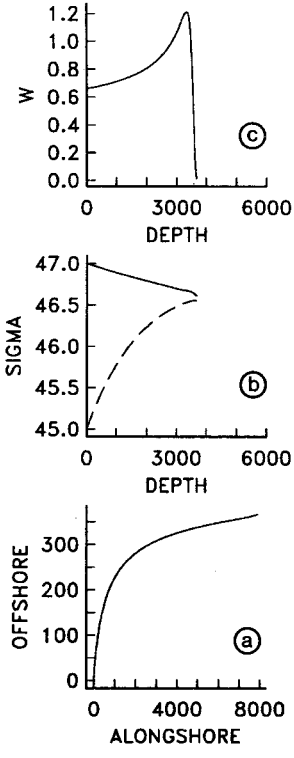

Fig. 4. Model solution for $\delta\rho = 0.04 \times 10^{-3}$ kg m^{-3}, twice the value used to obtain the solution in Fig. 3, all other parameters were left unchanged (a,b,c, as in Fig. 3).

magnitude of the horizontal velocities is proportional to w_z, and the southward velocity is significantly weaker than that of the bottom layer. A similar southward mid-depth circulation was calculated by TZIPERMAN (1986), although there it was a result of the somewhat arbitrarily specified shape of surface heating as a function of the surface density in water mass formation regions. GARGETT (1984) also found a southward mid-depth circulation by assuming an exponential density profile and then calculating the upwelling velocity profile using the density equation with a mixing coefficient which depended on the stratification.

The effect of variations in the entrainment and friction coefficients has been discussed thoroughly by SMITH (1975) and KILLWORTH (1977), and a complete review of the entrainment assumption is given by TURNER (1986). To illustrate the dependence of the profiles on the values of $\delta\rho$ and τ in the parameterization of detrainment, two additional solutions were calculated with different values. The solution is more sensitive to $\delta\rho$ than to τ, and the effect of doubling $\delta\rho$ is to smooth out the maximum in the profile of the interior vertical velocity (Fig. 4). Doubling $\delta\rho$ spreads out the distribution of densities in the boundary current at a given level, and allows fluid parcels to escape the boundary current over a broader depth range. Decreasing τ by a factor of 10 has no noticeable effect on the profile of the vertical velocity. The sole difference between this case and the original solution is a slightly reduced alongshore penetration of the boundary current.

Some solutions were obtained using an entrainment of the form $E_0 A^{1/2} Ri^{-1.7} V$, where $Ri = \Delta\rho/V^2$ is the Richardson number. The exponent of Ri is from TURNER (1973, Fig. 6.8). This changed the structure of the plume and hence the interior vertical velocity, but the basic increase of w with depth followed by its decrease still held—as it must for an entraining–detraining plume. Exponents of higher magnitude were tried, which confine the entrainment nearer the source and result in a smaller w_z at mid-depth.

Effect of rotation

In any buoyant plume, the density difference $\Delta\rho$ drives the motion. Without rotation, the dense fluid falls straight down the slope and is driven inward by a horizontal pressure gradient. With rotation, the density difference cannot drive the fluid inward directly because the Coriolis force can balance the buoyancy force and the motion is mostly along isobaths. Friction is necessary for the current to descend, and at the same time, rotation increases the path length giving friction more time to act.

A number of solutions were calculated with different rates of rotation, keeping all other parameters constant. As the rotation rate decreased, the initial density difference was reduced so that the two densities converged at 4000 m depth. Without rotation the path length of the plume is about a factor of 30 shorter (Fig. 5), which does not give the current time to build up its transport much above the initial value. The initial density difference, and hence overall stratification is roughly half that of the case with Earth's rotation (Fig. 3). A smaller density difference with fixed heat flux produces a greater initial transport and therefore greater upwelling. The depth scale d is now about 700 m. Owing to the flatness of the vertical velocity profile, the horizontal circulation is mostly confined to depths greater than 2000 m.

To see how the frictional dissipation may control the solution, suppose that the potential energy density of the plume is $gH\,\Delta\rho$, where H is the depth of the basin. The dissipation is the path integral of the drag, or $\int_0^{X_i} K_0 A^{1/2} V^2\, d\xi/A$. [Alternatively, approximate the

integral of (5) with initial values and note that $\int_0^{Xi} \tan(\alpha) \sin(\beta)\, d\xi = H$.] As a rough estimate approximate the dissipation by substituting the scaled values $K_0 = 0.1$, $A^{1/2} = 1$, and $V^2 = 0.1$. Setting the two estimates equal gives

$$H\Delta\rho = 0.01Xi.$$

As Xi rapidly increases with the rotation rate, this relation implies that $\Delta\rho$ increases with rotation. The terms $H\Delta\rho$, $0.01Xi$, and the numerically evaluated dissipation integral are plotted together in Fig. 6 for $H = 4$. The dissipation estimates are all larger than $H\Delta\rho$, although the numerical estimates are much closer than the simple relation given above at greater rotation rates. Based on these estimates, we suggest that the rotation increases stratification, to supply enough potential energy to overcome friction.

With vertical walls ($\alpha = \pi/2$) and no rotation, the path length is just the basin depth. Over such a short distance the entrainment and detrainment as formulated are too weak to have any effect on the current. The standard formulation of entrainment in this situation though, replaces $E_0 A^{1/2} V$ by $E_0 V$, with $E_0 = 0.255$ and sets $K_0 = 0$, since there is no longer a boundary to rub against. In this case solutions similar to MANINS (1979) were found. The density difference at 4000 m could be made as small as desired by reducing $\Delta\rho$, creating a correspondingly thin pycnocline, but as the plume never runs out of water there is no basis for settling on an initial value.

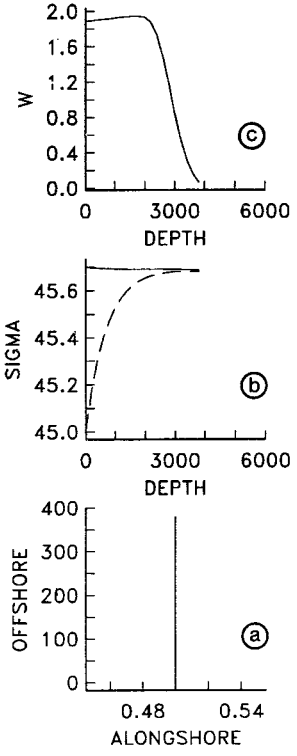

Fig. 5. Model solution for no rotation (a,b,c, as in Fig. 3).

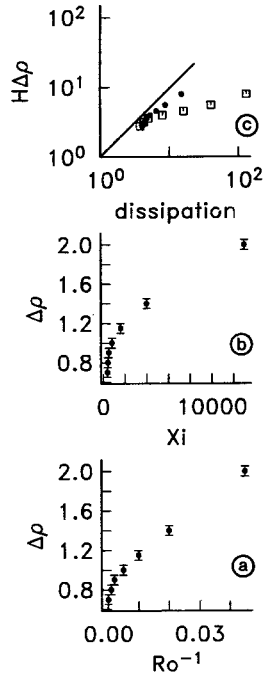

Fig. 6. (a) Initial density difference for different rotation ($f = 3.16 \times 10^{-3} R_0^{-1}\ s^{-1}$). (b) Density difference and path length Xi for different rotation rates. (c) Estimates of initial potential energy and dissipation (scaled by $g'L$). The line has a slope of one, 0.01 Xi (open squares), numerically integrated values (dots).

Topography

In a basin with sloping sides the interior area decreases with depth. To examine the effect of this on the vertical velocity profile the basin was assumed to be square in cross-section with each wall having the same slope $\alpha = 10^{-2}$ (Fig. 7). This is handled by putting $A_I = A_I(z)$ in the mass equation. However, if the total density flux equation (8) is derived in the same manner, an extra term appears representing the heat flux at the sloping boundary. To preserve the density balance in the basin, this term is neglected and the total density flux equation is used to calculate ρ_{ez} at each step.

The decrease of area with depth increases the upwelling proportionately (Fig. 8). The

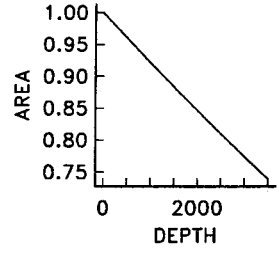

Fig. 7. Interior area vs depth.

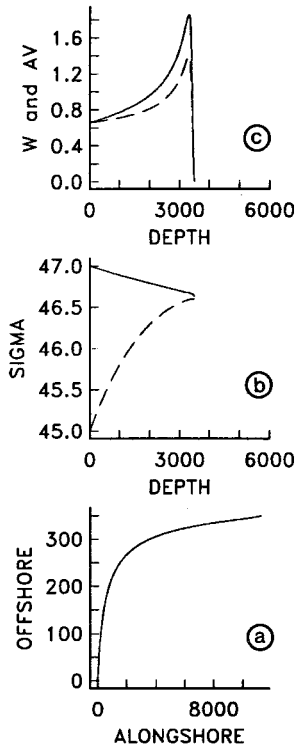

Fig. 8. Model solution with sloping side walls (a,b,c, as in Fig. 3).

vertical velocity varies more sharply with depth than before (Fig. 3) while the change in the density–depth curve is only a very slight upward shift.

In the ocean there is usually a continental rise of intermediate slope before reaching the more or less flat abyssal plain. This feature was represented in the model by reducing α to 5×10^{-4} at a depth of 2000 m. Then the area decreases below 2000 m to almost zero near the bottom. A solution was found without rotation; with earth's rotation the current is obliged to stay near the 2000 m isobath and could not make it to the required depth. The rapid decrease in area below 2000 m produces a tall peak in the vertical velocity profile, which shifts the density–depth curve upward near the bottom in an exaggerated version of the previous solution (Fig. 8). For special hypsometric forms, the area averaged vertical velocity could increase with depth all the way to the bottom.

4. DISCUSSION

There are several potentially interesting extensions of the present model that could be addressed by future work. In the ocean, the deep water in a given basin is often supplied by several sources (e.g. Norwegian Sea overflow, Mediterranean outflow, the Labrador Sea, and the Antarctic region are all sources of deep water for the Atlantic Ocean). It is possible to add several sources in the present model and examine their interaction with the interior and with each other. Another possible extension would be the separate treatment of

temperature and salinity in the model, relating them to the density field through an equation of state. SPEER and RONA (1989) used a model similar to the present one to investigate the effect of a deep geothermally driven plume on the T–S interior relation at the level where the plume loses its water to the interior and spreads horizontally along an isopycnal surface. Finally, the shallow wind-driven interior circulation is not explicitly included in the present model. TZIPERMAN (1986) found that horizontal variations in the thermocline depth resulting from the wind-driven circulation can influence the circulation in the layers below the thermocline. It may be interesting, therefore, to try and relax the assumption of flat isopycnal surfaces, especially in the upper part of the interior, and examine the corrections to the interior circulation.

MANINS (1979) discussed the two-dimensional convection problem with a point buoyancy source, and it is worthwhile at this point to discuss the differences between his approach and the present model. Aside from the lack of rotation in his model, a major difference is the treatment of the detrainment of the boundary current into the interior. The addition of the detrainment term (3) in the present model enables boundary current water to return to the interior when the densities match. In MANINS' (1979) work, the boundary current hits the lower boundary where its density is not necessarily equal to that of the interior. A density discontinuity is therefore formed at that place between heavy boundary current water and light interior water, and a thin boundary layer is needed to remove this discontinuity and return boundary current water to the interior. Manins did not explicitly solve for this layer, but derived its thickness and related scales. In the present model the detrainment of the boundary current water occurs in a continuous manner, with no density jump between bottom water and boundary current water.

We have used a simple model to demonstrate how the deep stratification and circulation of the oceans is determined by remote forcing at the surface, in regions of dense water formation. Using the large-scale linear vorticity equation, the interior flow was toward the south and west in the upper levels of the deep water, owing to the mass sink there, and toward the north and east in the lower levels where there is a mass source. These flows ought to feed and be supplied by their own set of boundary currents, which have been ignored in this study. The extent of the interior water column occupied by northward- or southward-flowing water may depend on the type of parameterization of mixing in the model. A simpler mixing scheme perhaps depending only on the Richardson number would be more satisfying.

Acknowledgements—Support for KGS came from NSF grant OCE85-15642 to T. Joyce and OCE82-13967 to B. Warren at WHOI, and also from the WHOI–MIT Joint Program Ocean Ventures Fund. Further support came from a grant from the Ministère des Affaires Étrangers while at IFREMER, Brest, France. A reviewer's questions led to the improvement of this report. WHOI Contribution no. 6917.

REFERENCES

BAINES W. D. and J. S. TURNER (1969) Turbulent buoyant convection from a source in a confined region. *Journal of Fluid Mechanics*, **13**, 51–80.

GARGETT A. E. (1984) Vertical eddy diffusivity in the ocean interior. *Journal of Marine Research*, **42**, 359–393.

GILL A. E. (1982) *Atmosphere–ocean dynamics*. International Geophysics Series, Vol. 30, Academic Press, New York, 662 pp.

KILLWORTH P. D. (1977) Mixing on the Weddell Sea continental shelf. *Deep-Sea Research*, **24**, 427–448.

MANINS P. C. (1979) Turbulent buoyant convection from a source in a confined region. *Journal of Fluid Mechanics*, **91**, 765–781.

SHAMPINE L. F., H. A. WATTS and S. DAVENPORT (1975) Solving non-stiff ordinary differential equations—the state of the art. Sandia Laboratories Report SAND75-0182, Sandia Laboratories, Albuquerque, New Mexico.

SMITH P. C. (1975) A streamtube model for the bottom boundary currents in the ocean. *Deep-Sea Research*, **22**, 853–874.

SPEER K. G. and P. A. RONA (1989) A model of an Atlantic and Pacific hydrothermal plume. *Journal of Geophysical Research*, **94**, 6213–6220.

STOMMEL H. and A. B. ARONS (1960) On the abyssal circulation of the World ocean—I. Stationary planetary flow patterns on a sphere. *Deep-Sea Research*, **6**, 140–154.

TURNER J. S. (1973) *Buoyancy effects in fluids*. Cambridge University Press, London, 367 pp.

TURNER J. S. (1986) Turbulent entrainment: the development of the entrainment assumption, and its application to geophysical flows. *Journal of Fluid Mechanics*, **173**, 431–471.

TZIPERMAN E. (1986) On the role of interior mixing and air–sea fluxes in determining the stratification and circulation of the oceans. *Journal of Physical Oceanography*, **16**, 680–693.

WARREN B. A. (1977) Shapes of deep density–depth curves. *Journal of Physical Oceanography*, **7**, 338–344.

WARRREN B. A. (1981) Deep circulation of the world ocean. In: *Evolution of physical oceanography, Scientific Surveys in Honor of Henry Stommel*, B. A. WARREN and C. WUNSCH, editors, The MIT Press, Cambridge, Massachusetts, pp. 6–41.

WORTHINGTON (1970) The Norwegian Sea as a Mediterranean basin. *Deep-Sea Research*, **17**, 77–84.

APPENDIX

Parameterization of detrainment in the bottom boundary current

It was assumed in the text that the density of the boundary current is uniform in cross-section. But one expects that there would be some density variations across a section of the current. Consider a slice of the tube, with thickness $d\xi'$, and with density as represented in the above model $\rho(\xi)$. Suppose that the actual density of water in the slice is distributed around the central value of ρ, so that there is water of density other than ρ present at every location along the current. Assuming an exponential distribution, the amount of water with density in the range $(\rho', \rho' + d\rho')$ present in the above slice is

$$M(\rho')\,d\rho'\,d\xi' = \left(\frac{A\rho_0}{2\delta\rho}\right) d\xi'\,d\rho' \exp\left(-\frac{|\rho - \rho'|}{\delta\rho}\right),$$

where A is the tube cross-section area, and $\delta\rho$ is the "width" of the density distribution in the slice (note that adding up the mass of water at all densities in the slice gives the total mass of the slice $\int_{-\infty}^{\infty} d\rho'[M(\rho')\,d\xi] = A\,d\xi'\rho_0$).

The mass of water particles in the slice with density less than or equal to the density of the interior water ρ_e is

$$\int_{-\infty}^{\rho_e} d\rho'[M(\rho')\,d\xi'] = \frac{A\rho_0}{2\delta\rho} d\xi' \exp\left(-\frac{|\rho - \rho_e|}{\delta\rho}\right).$$

As the slice of water moves down the sloped bottom, fluid particles whose density is now lighter than the interior density find their way to the edge of the tube, and are lost to the interior. Assume that a fluid particle of density lighter than the interior density takes an average time τ to find its way to the interior. The mass transport through a section of the current, per unit time is $\rho_0 AV$. Out of this,

$$\frac{\rho_0 AV}{2\delta\rho} \exp\left(-\frac{|\rho - \rho_e|}{\delta\rho}\right)$$

has a density lesser than or equal to the interior density at this level, ρ_e. Over a distance of $d\xi$, traveled by the current in a time $dt = d\xi/V(\xi)$, the current loses to the interior via detrainment a part dt/τ of the water with density lighter than ρ_e. This can be written as

$$(AV)|_{\xi+d\xi} - (AV)|_{\xi} = \frac{d(AV)}{d\xi} d\xi = \frac{dt}{\tau} \frac{AV\rho_0}{2\delta\rho} \exp\left(-\frac{|\rho - \rho_e|}{\delta\rho}\right).$$

Substituting dt, and adding the entrainment term, we find the form of P_M used in (1) and (3)

$$\frac{d(AV)}{d\xi} = E_0 A^{1/2} V - \frac{A\rho_0}{2\delta\rho\tau} \exp\left(-\frac{|\rho - \rho_e|}{\delta\rho}\right).$$

This is not meant to be a realistic parameterization of the complex mechanism of detrainment, but only to represent it in the model. The parameters τ and $\delta\rho$ were simply chosen to give "reasonable looking" results. This extension to the entrainment model used by SMITH (1975) and KILWORTH (1977) allows the boundary current to lose its water when reaching a level where its density is nearly equal to the interior density, and is therefore crucial to the model presented here.